The Pennsylvania State University
College of Earth and Mineral Sciences
Department of Materials Science and Engineering

Microhardness Analysis of the Cape York Meteorite

A Thesis in Materials Science and Engineering

By

Jeffrey S. Spedding

Submitted in Partial Fulfillment of the Requirements for the Degree of Bachelor of Science in Materials Science and Engineering (Metals Options).

12/10/2010

I approve this thesis: Date :
Signature:

Dr. Paul R. Howell, Professor of Metallurgy

Thesis Advisor

Abstract

An asteroid is an irregularly shaped body that orbit around the sun in a highly concentrated portion of the solar system located between Mars and Jupiter known as the asteroid belt. These asteroids were formed from dust particles, ice and gas clouds that formed every other body in the solar system, but they have not fully evolved into planets or were once planets that have been destroyed due to cataclysmic collisions. They follow a set trajectory or orbit that is most commonly seen in other celestial bodies such as planets. Occasionally these asteroids get knocked off their orbit and are sent on a collision course with earth. Once the asteroids come into contact with earth's surface they are then given a new name: meteorites.

Meteorites are very important for scientists because their structure was formed over billions of years of cooling. This structure is as close to equilibrium conditions with respect to phase transformations that can be studied.

This thesis focuses on the microhardness associated with the different phases that can be observed in the Cape York meteorite. It is also hopeful to show that there is a difference between martensite and Widmanstätten ferrite.

TABLE OF CONTENTS

ACKDOWLEDGEMENTS

First, I would like to thank Dr. Paul Howell and Prateek Dasgupta for their assistance and patience while working with me on this thesis. Without their help and guidance this thesis would not have been half of what it is. I also would like to thank everyone in the MATSE department for all the help that they have provided me with during my career at Penn State. I finally would like to thank my family and friends for their continued support and help in every aspect of my life.

LIST OF FIGURES

LIST OF TABLES

Chapter 1: Introduction

1.1 The Importance of Studying Meteorites

Meteorites have remained largely unchanged for billions of years. Many of them have the same composition as when the solar system was formed [1]. Through studying these meteorites we can gain insight on many topics including: the composition of other planets that they may have broken away from, aid in understanding how microstructures form under equilibrium cooling rates, as well as potentially updating phase diagrams based on the extremely low cooling rate associated with the asteroid's solidification and solid-state cooling. Studying meteorites also has the potential to give us a better understanding of space and the solar system as a whole. Understanding meteorites could increase space exploration through greater understanding of the conditions in space, provide a new resource possibility through mining potential, as well as potentially proving life exists on another planet.

1.1.1 Intent of Study

The meteorite that is going to be focused on in this thesis is the Cape York meteorite. More information is provided in section 2.3. The purpose of this study is to show that there is a difference in hardness between primary Widmanstätten ferrite, secondary Widmanstätten ferrite and martensite. This will be done through proper sample preparation, use of optical microscopy to identify the three structures and finally microhardness testing to prove the hypothesis stated above.

1.1.2 Metallurgical Benefits

The study of meteorites can assist metallurgist in many ways. One of the most crucial ways it can assist metallurgists is through the improvement of the iron-nickel phase diagram. Phase diagrams are meant to be made from experimental results that are gathered at near equilibrium conditions. These near equilibrium conditions could never be produced in a laboratory environment because of the extremely slow cooling and diffusion rates that need to be achieved. In meteorites, these rates lead to the closest thing to a perfect microstructure that can be analyzed. Meteorites have cooled at a rate of anywhere from 0.1 to 500 ^{o}C per million

years [2]. With further study of meteorites, a more accurate iron-nickel phase diagram can be produced and, in turn, lead to more efficient processing times yielding a more precise and desired microstructure.

1.1.3 Previous Meteorite Findings

Finding meteorites on earth has many benefits, some monetarily to the finder, but much more so to the scientific community as a whole. One such meteorite, named ALH84001, fell in Allen Hills Antarctica and was found in 1984. Several astonishing findings were found from this meteorite. These findings include "hydrocarbons which are the same as breakdown products of dead micro-organisms on Earth, it contained mineral phases consistent with by-products of bacterial activity, and tiny carbonate globules which may be microfossils of the primitive bacteria" [3].They also concluded that the rock originated from mars and solidified approximately 4.5 billion years ago [3]. This evidence for alien life is only one of the benefits that meteorites have to offer.

Studying meteorites can show many different things relating to everything from space's environment, other planets' environments, as well as how to better make steels for various applications. As a result, continuation of terrestrial projects to find meteorites as well as inter-solar system recovery projects need to continue to be funded.

1.2 Environmental Effects

In addition to all the implications meteorites could have on the current metallurgical processes they can also have a major effect on our environment. Meteorites hitting earth could have negligible effects or major consequences. Naturally, the larger the meteorite is, the more damage it will cause to earth. Table 1 shows the size of meteorites, the expected weight of the meteorite (in megatons), and the range of damage that can be expected from it's impact with earth.

Smaller meteorites will vaporize when they come into contact with the earth's atmosphere, however the larger ones will leave a noticeable crater. Larger meteorites will enter the earth's atmosphere at an average speed of between 10 and 70 kilometers per second. For

smaller to medium sized meteorites this speed will drastically reduce to several hundred kilometers per hour due to friction with earth's atmosphere [4]. For the largest meteorites their momentum will continue to carry them very rapidly through the atmosphere and will cause an impact zone referred to as a crater. One of the most severe meteorites to have hit earth is named SL9, which is believed to cause the extinction of the dinosaurs approximately 65 million years ago. It impacted earth near Chicxulub in the Yucatan Peninsula and left a crater approximately 180 kilometers in diameter [4]. As a result of these potentially devastating meteorites NASA has implemented a project which will detect meteorites with a trajectory which will hit earth or come extremely close to earth. This program is termed SENTRY. SENTRY is " a highly automated, accurate, and robust system for continually updating the orbits, future close Earth approaches, and Earth impact probabilities for all Near-Earth Asteroids (NEAs)" [5].

Table 1: The Destructive Possibilities of Meteorite Collision [4]

Impact Diameter (meters)	Yield (megatons)	Interval (years)	Consequences
< 50	< 10	< 1	Meteors in upper atmosphere don't reach surface
75	10 - 100	1000	irons make craters like Meteor Crater; stones produce airbursts like Tugska; Land impacts destroy area size of city
160	100 - 1000	5000	irons,stones hit ground; comets produce airbursts; land impacts destroy area size of large urban area (New York, Tokyo)
350	1000 - 10000	15000	land impacts destroy area size of small state; ocean impact produces mild tsunamis
700	10000 - 100000	63000	land impacts destroy area size of moderate state (Virginia); ocean impact makes big tsunamis
1700	100000 - 1000000	250000	land impact raises dust with global implication; destroys area size of large state (California, France)

Chapter 2: Literature Review

2.1 Formation and Origins of Meteorites

An asteroid is defined as any of the small rocky celestial bodies found especially between the orbits of Mars and Jupiter [6]. This specific location has been termed the asteroid belt due to the extremely high concentrations of asteroids that are orbiting in this region. Asteroids range in size from 1 to 800 km in diameter. The asteroid belt formation has been addressed in several theories. These theories include Laplace's nebular hypothesis and Bode's rule.

2.1.1 Laplace's Theory of Planetary Formation, Bode's Rule

Laplace's nebular hypothesis was published in 1796 and describes the steps in the formation of planets as well as the asteroid belt. The nebular hypothesis is made up of 7 steps that explain the process of planetary formation. Laplace's hypothesis is still supported by many scientists and has endured the test of time. Laplace's theory is as follows:

1. The sun was originally a giant cloud of gas or nebulae that rotated evenly.
2. The gas contracted due to cooling and gravity.
3. This forced the gas to rotate faster, just as an ice skater rotates faster when his extended arms are drawn onto his chest.
4. This faster rotation would throw off a rim of gas, which following cooling, would condense into a planet.
5. This process would he repeated several times to produce all the planets.
6. The asteroids between Mars and Jupiter were caused by rings which failed to condense properly.
7. The remaining gas ball left in the center became the sun [7].

Laplace was not the only scientist to mention or take into account the asteroid belt and its formation. Bode's rule was developed by J. E. Bode in 1775 which describes, or "predicts" the distance of a planet from the sun. Bode's rule is "a mathematical formula which generates, with

a fair amount of accuracy, the semi major axes of the planets in order out from the Sun. Write down the sequence

0, 3, 6, 12, 24…

And add 4 to each term:

4, 7, 10, 16, 28...

Then divide each term by 10. This leaves you with the series

0.4, 0.7, 1.0, 1.6, 2.8...

Which is intended to give you the semi major axes of the planets measured in astronomical units [8]".

This law is also given in the form of:

$$R = 0.4 \text{ A.U.} + 0.3*(2^n) \text{ A.U.}$$

A.U. stands for astronomical unit, or the mean distance from the sun [9]. This formula accurately predicts the locations of the planets (Mercury predicted: 0.4 A.U. Mercury actual: 0.39 A.U. Earth predicted: 1 A.U. Earth actual: 1 A.U.) as well as an anomalous prediction between Mars and Jupiter (located at 2.8 A.U.); this is where the asteroid belt is situated [10]. It has been theorized that the asteroids in the asteroid belt are the remnants from a planet that didn't form fully and to the constant collisions between the asteroids as well as the massive gravitational pull from Jupiter [9].

As stated before an asteroid is a celestial body, one that has not entered earth's atmosphere. An asteroid becomes a meteorite upon contact with earth. Specifically it is defined as "A stony or metallic mass of matter that has fallen to the earth's surface from outer space [11]".

2.2 Classification of Meteorites

Meteorites are divided into four major categories: chondrites, achondrites, stony irons and irons [12]. A chondrite is a stony meteorite which has a matrix that is composed of cement with fine grain dust, inclusions composed of nickel-iron grains, iron sulfides, and magnetite, as well as chondrules. Chondrules are millimeter sized spheres of previously melted minerals which have come together with other melted minerals to form a stony meteorite. These spheres directly condensed out of the solar nebula and have experienced one or more heating and cooling cycles [13]. This type of meteorite is believed to be one of the oldest structures in the solar system, dating to approximately 4.5 billion years old. Chondrites can be further classified into various subgroups of which the ordinary chondrite is the most common, representing 73.5% of observed falls [12]. Chondrites in general represent approximately 82 percent of total meteorite falls to earth.

Achondrites are stony meteorites that have no chondrules present and look very similar to igneous rocks found on earth. As a result they are very difficult to find unless they are seen falling from the sky. Due to their igneous nature achondrites are believed to be formed on different parent planets. These parent planets are incorporated into the classification of the achondrites [14]. The most recognizable classifications include Lunar (originating from the moon) and Nakhlites or Chassignite (originating from Mars), but eleven other classifications also exist. Achondrites make up only 7.8 percent of meteorite falls [12].

Stony irons are a mixture of iron-nickel alloys and other non-metallic constituents. These types of meteorites are normally classified into one of two major subgroups; pallasites, and mesosiderites [12]. Pallasites are made of olivine crystals that are located in an iron-nickel matrix. These meteorites form at the outermost core of differentiated asteroids and are believed to be very similar to the stones that form the boundary between earth's core and mantle [15]. Mesosiderites are "a complex structure of often chaotic consistencies of nickel-iron and breccia silicates, which consist of pyroxene, plagioclase and olivine" [15]. Mesosiderites are believed to have come from a large differentiated asteroid that has collided with another large differentiated asteroid. Stony irons in general are very rare and represent only 1.2 percent of meteorite falls [12].

Iron meteorites make up approximately 4.8 percent of meteorite falls [12]. Iron meteorites will be explained more thoroughly than the previous three examples because the focus of this thesis is on the Cape York meteorite, an iron meteorite. More information for the previous three types of meteorites can be found in reference [12]. Iron meteorites are made up of a crystalline iron-nickel alloy. Most iron meteorites are the core of a differentiated asteroid. Differentiation starts when dust and grains clump together to form a mass which is then is exposed to a period of intense heat within the first few million years of its existence. It is finished with a period of cooling that occurs over the next few hundred million years of the asteroid's existence [15,16]. The initial heating process came from radioactive elements which were decaying. This heat allowed the heavier elements (iron and nickel) to flow to the core of the asteroid, while all the lighter materials (silica liquid) would remain in the mantle or the crust. This process can be seen in figure 1.

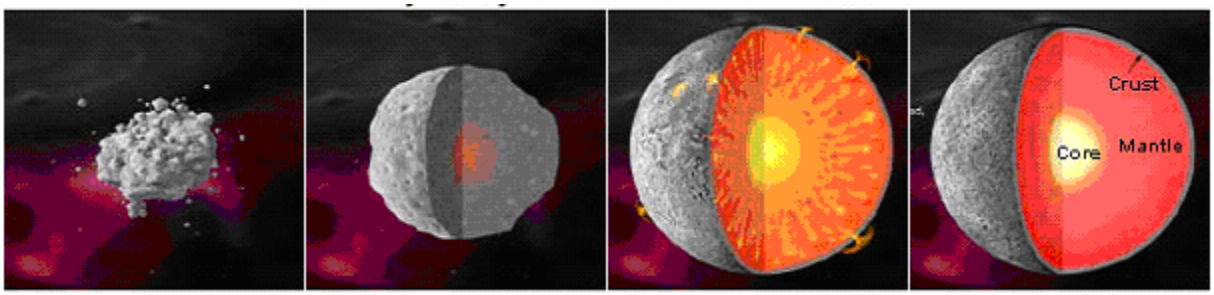

Figure 1: Schematic showing differentiation, formation of iron meteorites [16]

2.2.1 Classification of Iron Meteorites

Meteorites are classified either by using a chemical composition method, or a structural evaluation method [18]. The chemical composition method involves measuring trace amounts of metals such as germanium, gallium, iridium, tungsten and gold. The concentrations of these elements are then plotted against the overall concentration of nickel on a logarithmic scale. The results are then factored into one of 13 distinct groups designated with a roman numeral and letter combination. These groups can be seen in table 1. The individual groups are believed to have come from a common source, a unique differentiated asteroid that was broken apart by various collisions [19].

The structural evaluation method employs analyzing the meteorite for various structures that become apparent after proper specimen preparation [19]. Proper classification of iron meteorites depends on the size distribution of kamacite (ferrite) and taenite (austenite) within the microstructure. Iron meteorites can be placed into three categories using this method: hexahedrites, octahedrites, and ataxites [19].

Hexahedrites are primarily composed of kamacite, and are named for the arrangement of the crystal structure, in the form of a hexahedron. After etching, a hexahedrites sample will not exhibit a Widmanstätten pattern. However, they will display fine, parallel lines called Neumann lines. Both of these structures will be discussed in following sections [18].

Octahedrites are the most common structure exhibited by iron meteorites. A Widmanstätten pattern in an octahedrite shows an intergrowth of larger kamacite and taenite plates. This intergrowth is in the form of an octahedron, hence the name octahedrite. The spaces between the kamacite and taenite plates are filled by a fine grained mixture of kamacite and taenite termed plessite (discussed further in following sections). The octahedrites are divided into several subgroups based on their kamacite lamellae width. These subgroups can also be seen in table 1 along with their comparable group from chemical classification [18].

Ataxites generally don't show any obvious internal structure. They are primarily made up of nickel rich taenite with kamacite only being found in the form of microscopic lamellae and spindles. Ataxites make up the most nickel rich meteorites as well as the rarest meteorites recovered [18].

Table 2: Classification of Iron Meteorites [17,18]

Structural Class	Symbol	Kamacite (mm)	Nickel (%)	Related Chemical Groups
Hexahedrites	H	> 50	4.5 - 6.5	IIAB, IIG
Coarsest Octahedrites	Ogg	3.3 - 50	6.5 - 7.2	IIAB, IIG
Coarse Octahedrites	Og	1.3 - 3.3	6.5 - 8.5	IAB, IC, IIE, IIIAB, IIIE
Medium Octahedrites	Om	0.5 - 1.3	7.4 - 10	IAB, IID, IIE, IIIAB, IIIF
Fine Octahedrites	Of	0.2 - 0.5	7.8 - 13	IID, IICH, IIIF, IVA
Finest Octahedrites	Off	<0.2	7.8 - 13	IIC, IIICK
Plessitic Octahedrites	Opl	<0.2 , spindles	9.2 - 18	IIC, IIF
Ataxites	D	-	> 16	IIF, IVB

2.2.1.1 Phases in iron meteorites

A. Kamacite

Kamacite (ferrite) is a solid solution made up of ferritic iron with up to 7.5% Ni and can have up to 0.06 weight percent phosphorous. The nickel atoms in the solid solution substitute for the iron atoms in a body centered cubic lattice. The phosphorous atoms can substitute for either the nickel or iron atoms. Kamacite first starts growing around foreign inclusions that act as heterogeneous nuclei. At lower temperatures (50 – 100˚C) the kamacite have grown sufficiently large and will transform into the Widmanstätten structure (discussed further in following sections). Mechanical, plate-shaped twin lamellae termed Neumann bands are also found within the kamacite. They will occur in hexahedrites, octahedrites, and ataxites as long as there is a coherent kamacite phase which is 20-50 µm or greater in width. Neumann bands can range in size from 1 to 10 µm depending on the purity of the kamacite region. Neumann bands can form on 12 different planes because the twin plane is {211}α. Figure 2 shows a characteristic image of kamacite along with taenite (discussed in subsequent sections)[20].

B. Taenite

Taenite (Austenite) is a solid solution of face centered cubic austenite with more than 25% nickel present. Taenite has a range of compositions: nickel (25-50%), cobalt (0.3 – 0.8%), carbon (0.05 – 0.5%), and phosphorous (0.05 – 0.1%). Taenite is also significantly harder than kamacite. Figure 2 shows an image of taenite and kamacite [20].

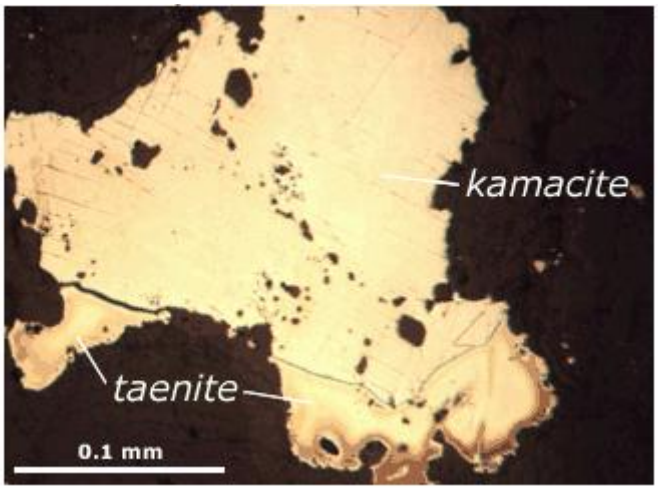

Figure 2: Image showing kamacite and taenite [21]

C. Inclusions

Inclusions occur in meteorites. These inclusions are equivalent to terrestrial inclusions. Several inclusions that are found in meteorites include cohenite, haxonite, carlsbergite, troilite, schreiberscite and rhabdite, and plessite.

Cohenite, $(Fe, Ni, Co)_3$, has an orthorhombic crystal structure and is closely related to cementite (Fe_3C). Cohenite contains 0.7 – 2.3% nickel and 0.02 – 0.3% cobalt [20].

Haxonite, $(Fe, Ni, Co)_{23}C_6$,has a cubic crystal structure and is closely related to $M_{23}C_6$. Haxonite contains 3.5 – 5.6% nickel and 0.05 – 0.4% cobalt [20].

Carlsbergite, CrN, has a cubic crystal structure and is found in small oriented laths in kamacite and as irregular grains in low ample grain boundaries. Carlsbergite is similar to corresponding precipitates found in steel [20].

Troilite, FeS, has a hexagonal crystal structure and is strongly anisotropic. Other elements may be found in troilite (nickel, cobalt, copper, chromium, manganese, zinc, lead) however they are virtually non-existent and composition can be estimated to be less than 1% [20].

Schreiberscite and rhabdite, $(Fe, Ni)_3P$, have a tetragonal crystal structure and do not have comparable terrestrial counterparts. The composition of schreiberscite and rhabdite are variable, however they have low nickel contents (10 – 15%) [20].

Plessite is a term that is defined as a mixture of both kamacite and taenite phases. Plessite is the last two-phase mixture to develop from the retained taenite. Plessite is usually encompassed by a taenite rim and usually form concave lines towards adjacent kamacite. There are various forms that plessite can take. These forms include: pearlitic, spheroidized, acicular, comb, net, cellular, finger, black, duplex, degenerated, and altered. Pearlitic plessite is used to describe a lamellar intergrowth. The lamellae are usually 0.5 – 2 μm wide. Spheroidized plessite is made 1 – 20 μm spherical taenite particles which are unevenly dispersed in a kamacite bulk. Acicular plessite has retained taenite with a "basket weave" intergrowth of kamacite platelets. Comb plessite have thin taenite ribs which come out of a continuous taenite frame. These ribs also indicate the bulk Widmanstätten orientations. Net plessite is very similar to comb plessite; however, the net form is sometimes just a section perpendicular to the comb plessite form. Cellular plessite is a mixture of kamacite grains in a taenite bulk. Finger plessite has a strong Widmanstätten orientation and is similar to cellular plessite. Black plessite is a term that is used for small wedge-shaped fields that appear black even after light-etching with nital. Duplex plessite are terms for transition zones in large plessite fields. A composition of 12 – 18% nickel is average for this zone. Degenerated plessite describes several forms, most commonly the comb, net, and cellular forms, which are imperfectly developed. This happens because there is not enough nickel in the meteorite and most of the taenite has disappeared after full primary cooling. Altered plessite is used to describe any form which has been modified in some manner through secondary, imperfect reheating [20]. Figure 3 shows a general plessite bounded by taenite as well as kamacite on the same micrograph.

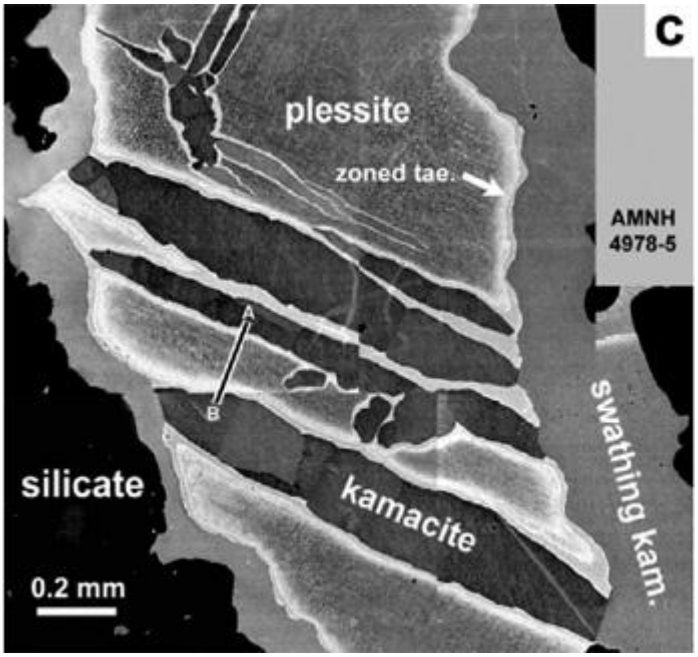

Figure 3: Image showing kamacite and plessite [22].

2.2.2 Structure of Iron Meteorites

A. Widmanstätten Structure

The Widmanstätten structure is a major characteristic for iron meteorites, more specifically octahedrites. It can also be found in terrestrial alloys such as cast brasses, welded joints in steels and tempered aluminum-silver alloys. In 1904 it was found that the Widmanstätten structure had to have formed at least 700˚C below the melting temperatures, a range between 700 and 450˚C. The process for forming this structure was found to be diffusion controlled nucleation and growth that is incredibly slow (on the order of 0.1 to 500 C per million years) [8, 19]. The Widmanstätten structure has a parent taenite (austenite) phase and kamacite (ferrite) which preferentially nucleates along the octahedral planes {111}. The structure is developed further when the individual plates of kamacite thicken and eventually conjoin. Some wedges or platelets are also retained in the structure and these are the high nickel taenite precursors which almost remain in some portion. Plessite is also present in the Widmanstätten structure; having a composition of between 6 and 20% nickel. Figure 4 shows the characteristic Widmanstätten structure [20].

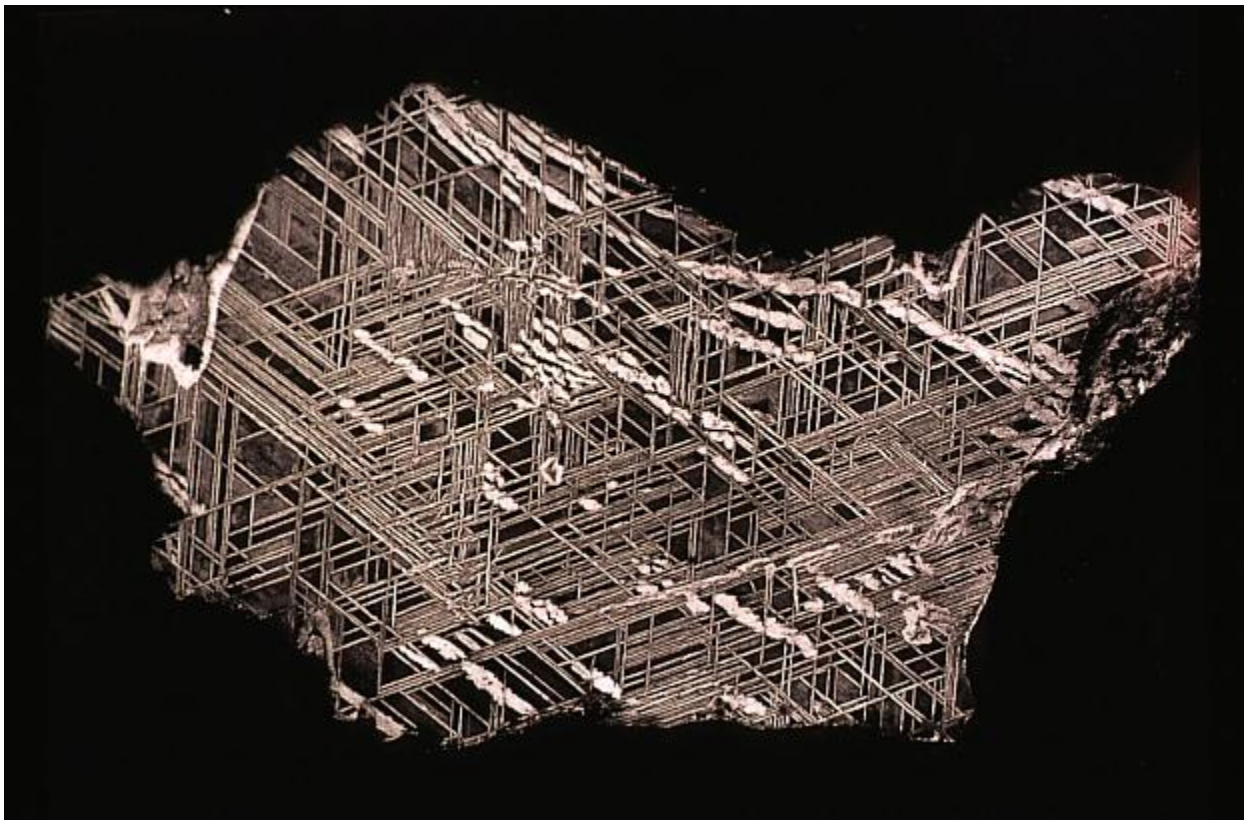

Figure 4: The characteristic Widmanstätten structure [23]

B. Martensite

Martensite is a microstructure which is common to steels. It is most commonly formed from a rapid quench of the austenite microstructure. This quenched FCC lattice of austenite is distorted to the body centered tetragonal structure of martensite. Martensite is very similar to ferrite; however, the subtle differences make it much stronger. The largest difference is that the carbon atoms get stuck in the austenite form when it is quenched and causes the perfect cube would be ferrite to be slightly elongated in one dimension and slightly shorter in the other two. These distortions yield a high dislocation density throughout the entire structure, vastly strengthening the material. The martensite structure can be characterized by the needle looking crystals. An example of this microstructure can be seen in figure 5 [24].

Martensite can also form in another manner as seen in meteorites. It can form at a low temperature below the martensite start temperature, M_s. Below this temperature the

martensitic reaction begins during cooling when austenite, the parent phase, reaches the M_s temperature. Below this temperature the austenite phase becomes mechanically unstable and it transforms rapidly to martensite. After this transformation no further transformations will occur. At constant decrease of temperature the austenite will continue to fall into a mechanically unstable region and more of it will transform to the martensite phase. This reaction will continue until the martensite finish temperature (M_f) is reached. After this point no more austenite will be converted to martensite via the mechanism described above [25].

Martensite also can be formed by the application of stress into the system. This formation of martensite however, is most commonly seen and used in the formation of toughened ceramics (most common example is in yttrium stabilized zirconium) and in specialty steels such as transformation induced plasticity steels [25].

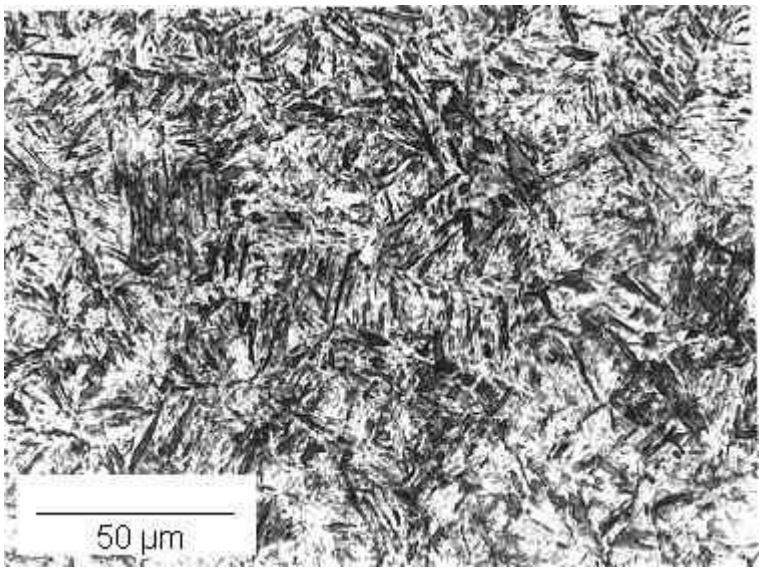

Figure 5: Characteristic martensitic structure [24]

2.3 The Cape York Meteorite

The meteorite that is going to be focused on in this thesis is the Cape York meteorite. This meteorite is thought to have struck earth 10,000 years ago. It was discovered on Saviksoah Island (which is off Greenland's Cape York) by Admiral Robert E Peary in 1894. For hundreds of years before the discovery of the Cape York meteorite, the native people of Greenland used the

meteorite as a source of iron for various applications including tools, and weapons. This meteorite was initially found to have broken up into 3 parts of 1000 pounds or more. These pieces were named Ahnighito (the tent) (31 tons), the “woman” (2.5 tons), and the “dog” (1000 pounds) by the natives. Multiple years later other masses have been found and one of them is believed to be “the man” from native legend [26].

The Cape York meteorite is classified as an IIIAB medium octahedrite meteorite. It has the following composition: 7.58% Ni, 19.2 parts per million gallium, 36.0 parts per million germanium, and 5.0 parts per million iridium.

Figure 6: Large samples of the Cape York Meteorite [27]

Chapter 3: Experimental Procedure

3.1 Sample Preparation

The sample that I was given of the Cape York meteorite was already mounted; however, the sample still needed to be properly polished and etched. The polishing procedure started by grinding the sample with sandpaper of grit sizes 400, 600, 800, 1200. The sample was then

polished further with a 0.3 µm alpha alumina slurry mixture on an Allied High Tech Productions Inc. Automatic Polisher. Upon completion of the polishing techniques the sample was flushed with distilled water and dried with an industrial hand dryer to prepare the surface for etching. The sample was then etched using a 2% Nital solution (composed of 2% nitric acid and 98% ethanol) for approximately 15 seconds. Once again the sample was flushed with distilled water and dried. Upon completion of the etching the sample was ready for optical microscopy and subsequent microhardness tests.

3.2 Optical Microscopy

Optical microscopy was used extensively in this experiment, specifically bright field optical microscopy. This technique was used to capture images which would allow for specific regions of the meteorite to be targeted for microhardness testing. Images were taken on a Zeiss Axiovert 200 MAT Optical Microscope. This microscope can be seen in figure 7. The Zeiss Axiovert 200 MAT Optical Microscope was used to collect images of the entire surface of the sample. These images were then assembled into a montage as can be seen in figure 10.

Figure 7: Image of Zeiss Axiovert 200 MAT used to collect images of the Cape York meteorite.

3.3 Vickers Hardness

The microhardness tests that were carried out on the sample were measured using the Vickers hardness scale. The Vickers hardness scale was developed in 1934 by Smith and Sandland at Vickers Ltd as an alternative test for the Brinell Method [28]. The Vickers hardness

test is a test which consists of an indenter which is associated with an equation which relates the diagonal widths of the square indent and the load pressure to a hardness value. The indenter is in the form of a right pyramid with a square base and angles of 136 degrees between opposite faces. An illustration of this can be seen in figure 8. When ready for a hardness test, a load is applied and the indenter leaves a square shaped imprint in the surface of the substance. This square has diagonals which are measured as D1 and D2 [29]. This representation can also be seen in figure 8.

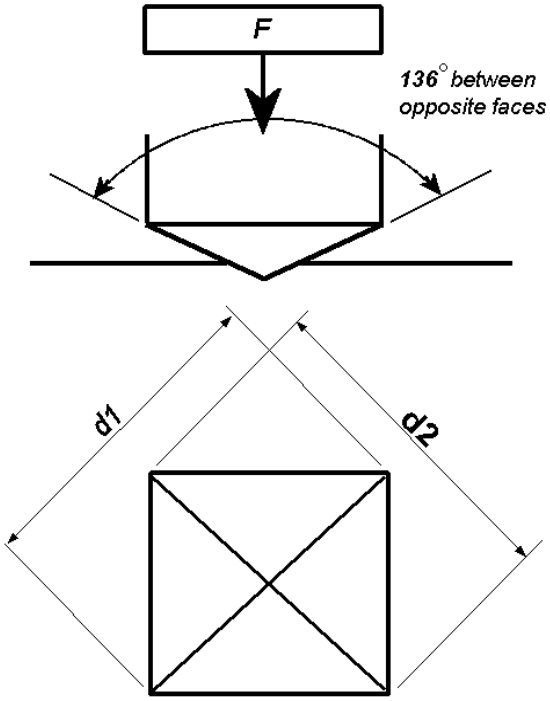

Figure 8: Representation of the Vickers hardness indenter and the characteristic square imprint with diagonals D1 and D2.

These factors are then put into Eq. 1 for calculation of the hardness value. HV is the Vickers hardness of the material, F is the force associated with the load on the indenter (in kilograms force), and d is the mean of the two diagonals, D1 and D2 [29].

$$HV = \frac{2F\sin\frac{136^{o}}{2}}{d^{2}} \qquad HV = 1.854\frac{F}{d^{2}} \text{ approximately}$$

Eq. 1

Each Vickers hardness test usually takes between 15 – 20 seconds, because the full load which is applied, has a normal dwell time of between 10 to 15 seconds. The experimenter also must be careful not to test within 2.5 indention diameters between samples. This is because the results may be skewed as a result of running into cold work resulting from a previous test [29]. The indenter used in this experiment was the Leco MHT Series 2000 Vickers Hardness Tester. This machine was used to test the primary Widmanstätten ferrite, secondary Widmanstätten ferrite, and martensite regions within the Cape York meteorite. An image of this machine can be seen in figure 9.

Figure 9: The Leco MHT Series 2000 Vickers Hardness Tester used to measure hardness values associated with various microstructures within the Cape York Meteorite

Chapter 4: Results

4.1 Optical Microscopy

Bright field optical microscopy was used to gather images of the surface of the Cape York Meteorite in order to find suitable locations for microhardness testing. The first step to finding appropriate locations was to compile a montage of the surface of the sample. This

montage can be seen in figure 10. Several locations were identified as being primary Widmanstätten ferrite, secondary Widmanstätten ferrite, and martensite. These locations would be focused on during subsequent hardness testing.

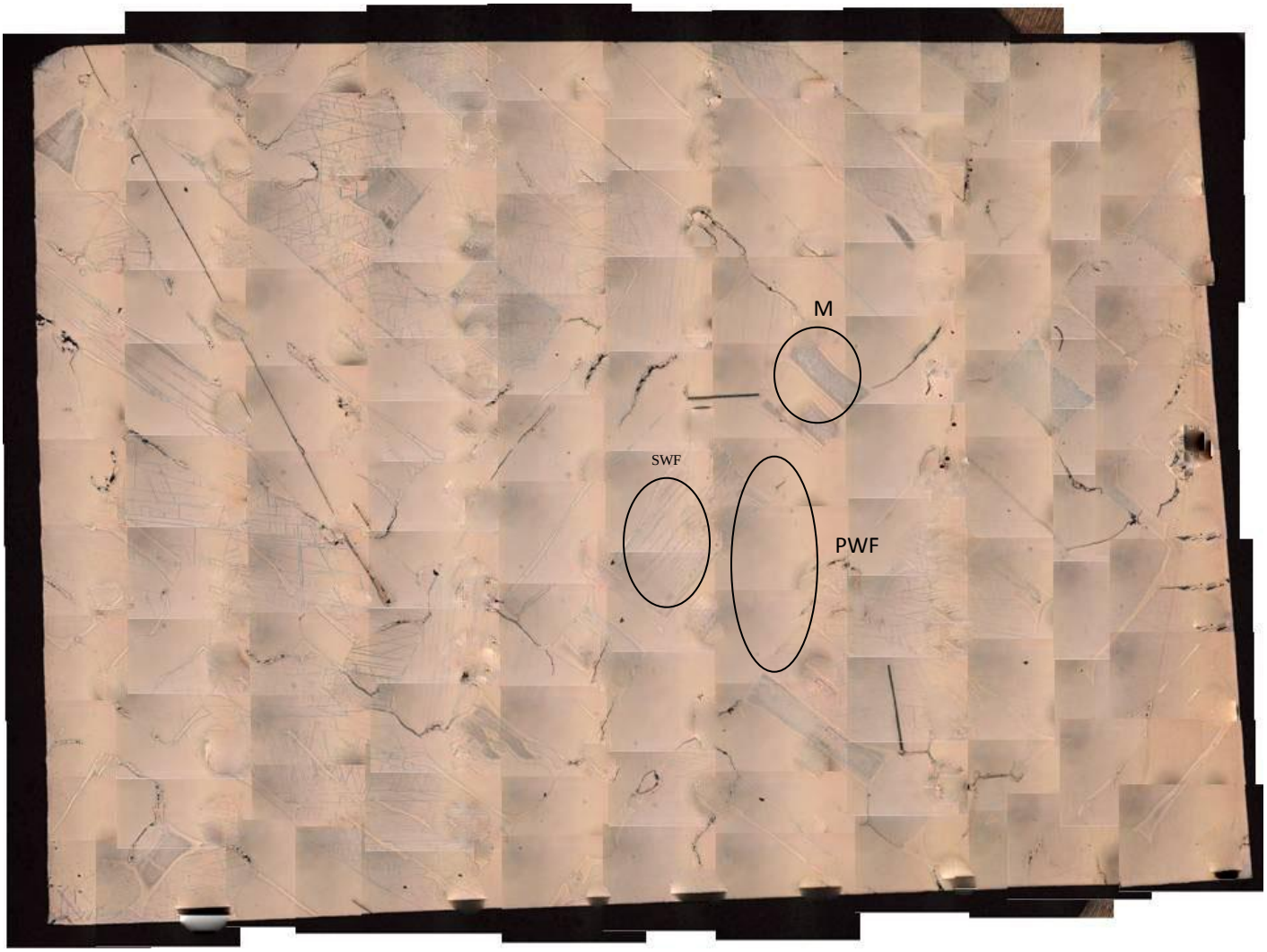

Figure 10: Montage of the Cape York Meteorite showing primary Widmanstätten ferrite (PWF), secondary Widmanstätten ferrite (SWF), and martensite (M).

4.2 Vickers Microhardness Testing

Vickers microhardness testing was carried out the primary Widmanstätten ferrite, secondary Widmanstätten ferrite, and martensite phases as observed in figure 10. In order to

increase the data field and to verify its accuracy several additional areas were identified and tested. The results from these tests are compiled into a series of tables showing the indention (test) number, the D1, D2 and $D_{average}$ values (in µm), the Vickers hardness associated with these results, and the mean and standard deviation of all of the results. Table 3 shows the data from martensite testing, table 4 shows the data from primary Widmanstätten ferrite testing, and table 5 shows the data from secondary Widmanstätten ferrite testing.

Table 3: Data From Martensite Microhardness Testing

Indention Number	Vickers Hardness	D1 (µm)	D2 (µm)	D avg (µm)
1	374	15.91	15.59	15.75
2	379	15.91	15.39	15.65
3	410	14.68	15.39	15.035
4	389	15.5	15.39	15.445
5	394	15.3	15.39	15.345
6	360	15.91	16.21	16.06
7	379	15.7	15.59	15.645
8	394	15.3	15.39	15.345
9	369	15.91	15.8	15.855
10	360	16.31	15.8	16.055
11	405	15.3	14.98	15.14
12	374	15.7	15.8	15.75
13	405	15.09	15.18	15.135
14	416	14.68	15.18	14.93
15	410	15.3	14.77	15.035
16	389	15.5	15.39	15.445
17	360	16.11	16	16.055
18	410	14.89	15.18	15.035
19	394	15.09	15.59	15.34
20	399	15.09	15.39	15.24
21	379	15.5	15.8	15.65
22	379	15.7	15.59	15.645
23	416	14.89	14.98	14.935
24	379	15.7	15.59	15.645
25	416	14.89	14.98	14.935

26	379	15.7	15.59	15.645
27	346	16.31	16.41	16.36
28	384	15.5	15.59	15.545
29	384	15.7	15.39	15.545
30	342	16.31	16.62	16.465
31	326	17.33	16.41	16.87
32	293	17.54	18.05	17.795
33	283	17.54	18.67	18.105
34	300	17.33	17.85	17.59
35	326	16.52	17.23	16.875
36	364	15.5	16.41	15.955
37	374	15.7	15.8	15.75
38	379	15.3	16	15.65
39	479	14.07	13.75	13.91
40	479	13.87	13.95	13.91
41	389	15.5	15.39	15.445
42	374	15.91	15.59	15.75
43	379	15.7	15.59	15.645
44	399	15.5	14.98	15.24
45	369	15.7	16	15.85
46	465	14.07	14.16	14.115
47	446	14.48	14.36	14.42
48	446	14.89	13.95	14.42
49	360	15.91	16.21	16.06
50	374	15.7	15.8	15.75
51	351	16.31	16.21	16.26
52	314	17.33	17.03	17.18
53	364	15.91	16	15.955
54	330	16.92	16.62	16.77
55	310	17.33	17.23	17.28
56	334	16.52	16.82	16.67
57	220	21.2	19.9	20.55
58	280	17.94	18.46	18.2
59	286	18.35	17.64	17.995
60	310	16.92	17.64	17.28
61	310	17.13	17.44	17.285
62	289	17.33	18.46	17.895
63	203	21.81	20.92	21.365
64	296	16.92	18.46	17.69
65	290	18.55	17.23	17.89
66	280	18.35	18.05	18.2

67	296	17.74	17.64	17.69
68	274	18.76	18.05	18.405
69	289	17.33	18.46	17.895
70	290	18.55	17.23	17.89
Mean	358.4857143	16.2377	16.2511	16.244429
Std Deviation	55.85974747	1.45343	1.39375	1.3956474

Table 4: Data From Primary Widmanstätten Ferrite Microhardness Testing

Indention Number	**Vickers Hardness**	**D1 (µm)**	**D2 (µm)**	**D avg (µm)**
1	226	20.18	20.31	20.245
2	217	21.41	19.9	20.655
3	231	20.18	19.9	20.04
4	220	21	20.1	20.55
5	229	21.2	19.08	20.14
6	215	21.41	20.1	20.755
7	217	21.41	19.9	20.655
8	217	21.41	19.9	20.655
9	217	21.41	19.9	20.655
10	228	19.98	20.31	20.145
11	228	19.98	20.31	20.145
12	231	18.96	21.13	20.045
13	238	18.96	20.51	19.735
14	243	19.16	19.9	19.53
15	233	19.16	20.72	19.94
16	238	18.76	20.72	19.74
17	233	19.57	20.31	19.94
18	236	18.96	20.72	19.84
19	237	20.3	19.23	19.765
20	250	20.3	18.2	19.25
21	250	20.3	18.2	19.25
22	264	19.27	18.2	18.735
23	264	19.27	18.2	18.735
24	264	19.27	18.2	18.735
25	250	20.3	18.2	19.25
26	296	18.24	17.17	17.705
27	264	19.27	18.2	18.735
28	279	18.24	18.2	18.22
29	279	18.24	18.2	18.22

30	264	18.24	19.23	18.735
31	264	19.27	18.2	18.735
32	250	19.27	19.23	19.25
33	264	18.24	19.23	18.735
34	264	18.24	19.23	18.735
35	279	17.21	19.23	18.22
36	279	18.24	18.2	18.22
37	279	18.24	18.2	18.22
38	279	17.21	19.23	18.22
39	279	18.24	18.2	18.22
40	250	18.24	20.26	19.25
41	279	18.24	18.2	18.22
42	279	17.21	19.23	18.22
43	279	18.24	18.2	18.22
44	264	19.27	18.2	18.735
45	296	17.21	18.2	17.705
46	264	18.24	19.23	18.735
47	296	17.21	18.2	17.705
Mean	253.2340426	19.199149	19.18766	19.193404
Std Deviation	24.08969901	1.2507404	0.9903935	0.9193861

Table 5: Data From Secondary Widmanstätten Ferrite Microhardness Testing

Indention Number	**Vickers Hardness**	**D1 (µm)**	**D2 (µm)**	**D avg (µm)**
1	259	18.15	19.69	18.92
2	243	18.96	20.1	19.53
3	248	18.35	20.31	19.33
4	251	18.35	20.1	19.225
5	236	19.78	19.9	19.84
6	213	20.79	20.92	20.855
7	209	21	21.13	21.065
8	207	21.2	21.13	21.165
9	222	20.59	20.31	20.45
10	236	19.98	19.69	19.835
11	226	20.79	19.69	20.24
12	229	20.59	19.69	20.14
13	220	21	20.1	20.55
14	211	21.41	20.51	20.96
15	243	19.98	19.08	19.53
16	215	21.2	20.31	20.755

17	209	21.81	20.31	21.06
18	207	21.61	20.72	21.165
19	217	21	20.31	20.655
20	215	21	20.51	20.755
21	220	21	20.1	20.55
22	224	20.59	20.1	20.345
23	222	20.39	20.51	20.45
24	217	21.2	20.1	20.65
25	211	21.2	20.72	20.96
26	222	20.59	20.31	20.45
27	211	20.79	21.13	20.96
28	220	21	20.1	20.55
29	219	20.59	20.51	20.55
30	213	21	20.72	20.86
31	219	20.79	20.31	20.55
32	224	20.79	19.9	20.345
33	219	20.39	20.72	20.555
34	215	21.2	20.31	20.755
35	222	21	19.9	20.45
36	217	20.59	20.72	20.655
37	207	21.2	21.13	21.165
38	203	21.2	21.54	21.37
39	217	20.39	20.92	20.655
40	211	20.79	21.13	20.96
41	217	20.39	20.92	20.655
42	213	19.98	21.74	20.86
43	219	19.78	21.33	20.555
44	215	20.39	21.13	20.76
45	217	20.39	20.92	20.655
46	213	20.79	20.92	20.855
47	228	20.18	20.1	20.14
48	211	21	20.92	20.96
49	201	21	21.95	21.475
50	205	20.79	21.74	21.265
51	233	19.98	19.9	19.94
52	215	21	20.51	20.755
53	207	21	21.33	21.165
54	219	20.79	20.31	20.55
55	207	21.2	21.13	21.165
56	215	21.41	20.1	20.755
57	209	21	21.13	21.065

58	238	19.37	20.1	19.735
59	207	21.61	20.72	21.165
60	199	21.41	21.74	21.575
61	213	21	20.72	20.86
62	224	19.37	21.33	20.35
63	199	21.41	21.74	21.575
64	211	20.79	21.13	20.96
65	207	21.61	20.72	21.165
66	203	21.2	21.54	21.37
67	211	20.39	21.54	20.965
68	205	20.39	22.15	21.27
69	203	21.2	21.54	21.37
70	197	21.2	22.15	21.675
Mean	217.2857143	20.6607143	20.69414286	20.677429
Std Deviation	12.46111966	0.74897867	0.664596408	0.5669022

Figures 11 through 16 show the indents formed by the microhardness testing in various microstructures.

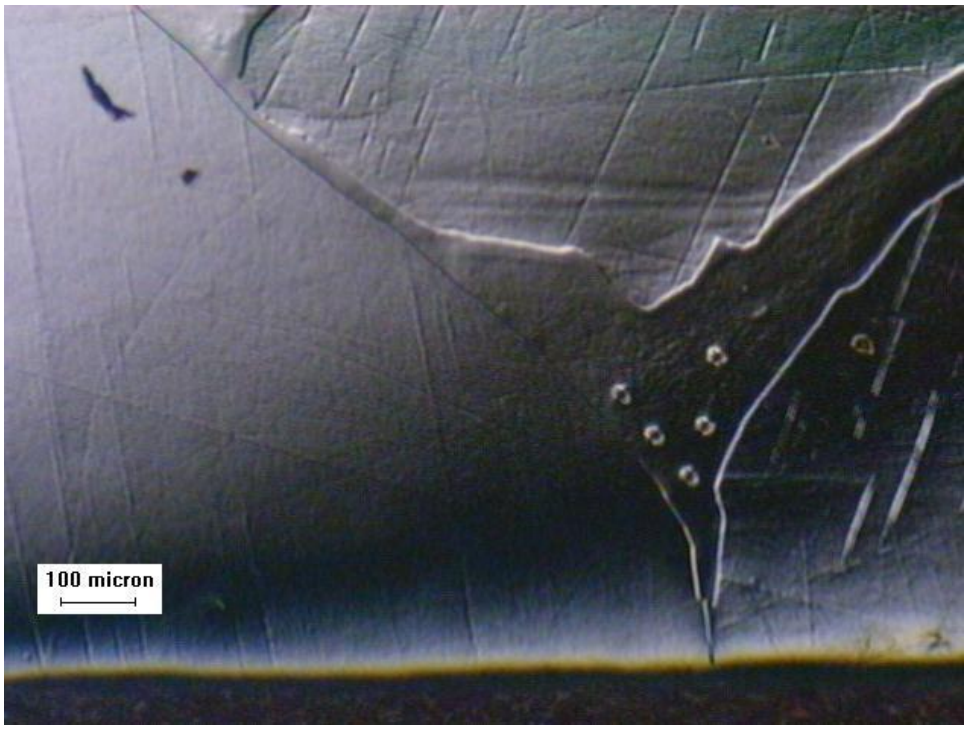

Figure 11: Vickers Hardness testing indents as seen on a martensite microstructure at 100x magnification

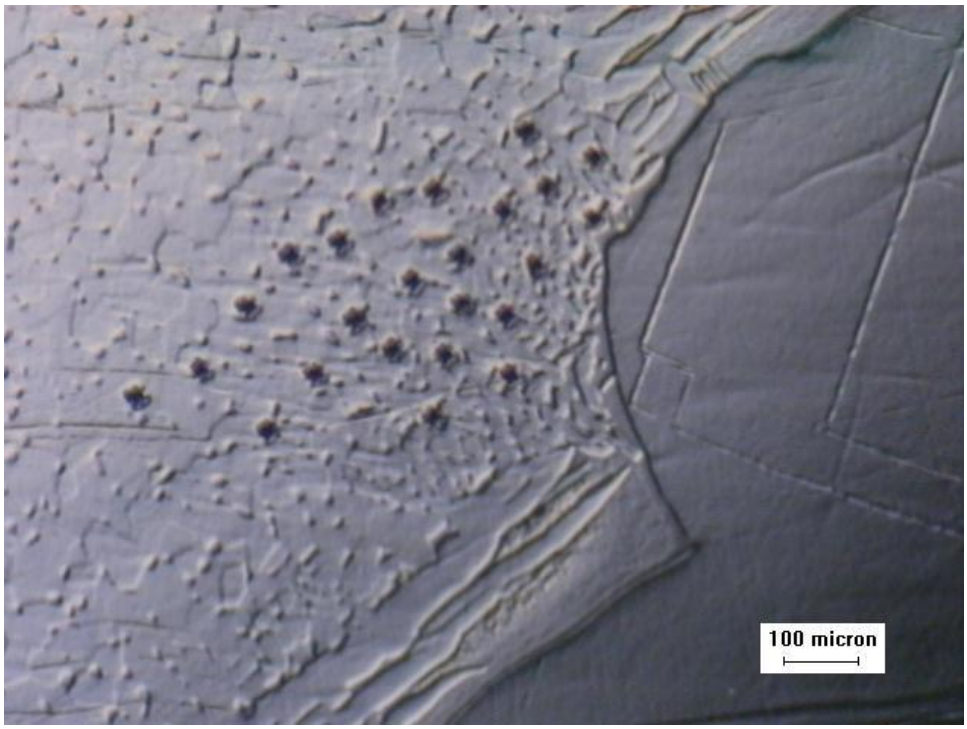

Figure 12: Vickers Hardness testing indents as seen on a martensite microstructure at 100x magnification

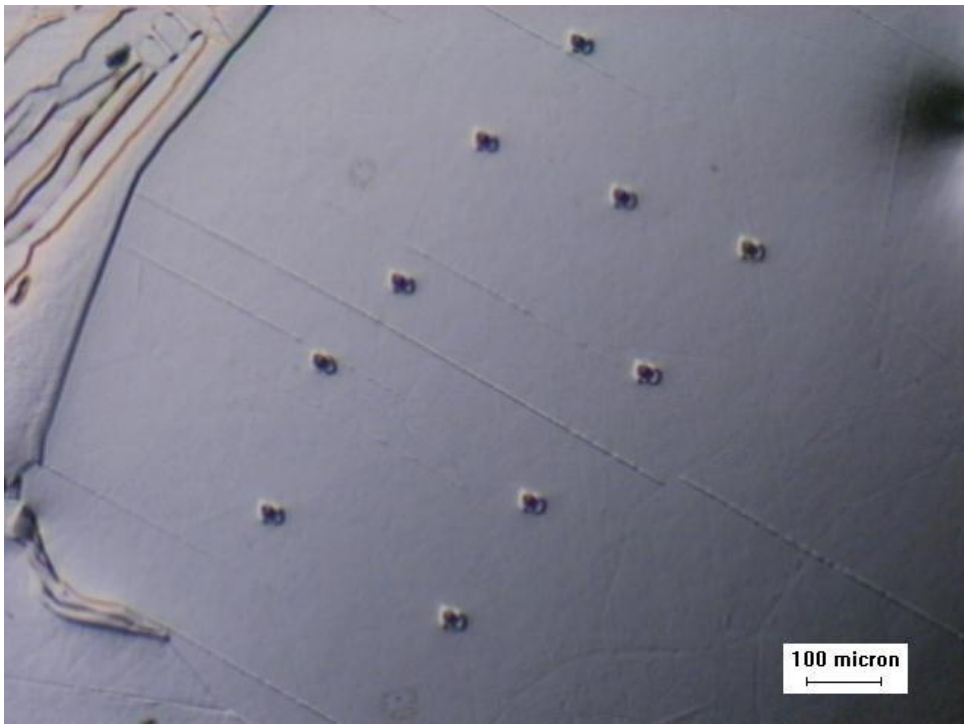

Figure 13: Vickers Hardness testing indents as seen on a primary Widmanstätten ferrite plate at 100x magnification

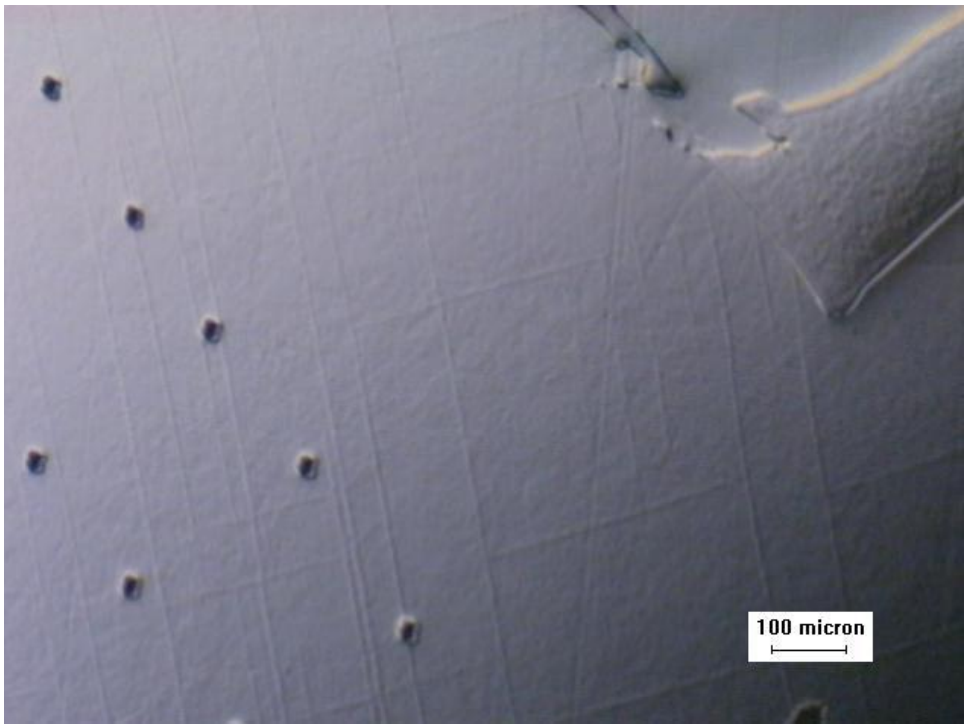

Figure 14: Vickers Hardness testing indents as seen on a primary Widmanstätten ferrite plate at 100x magnification

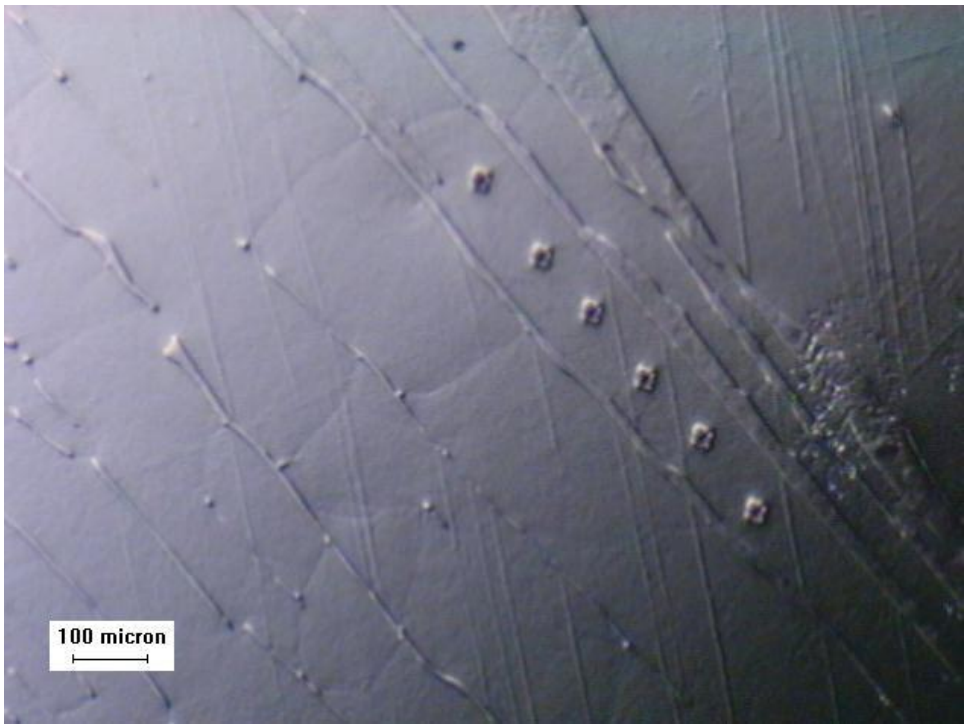

Figure 15: Vickers Hardness testing indents as seen on a secondary Widmanstätten ferrite plate at 100x magnification

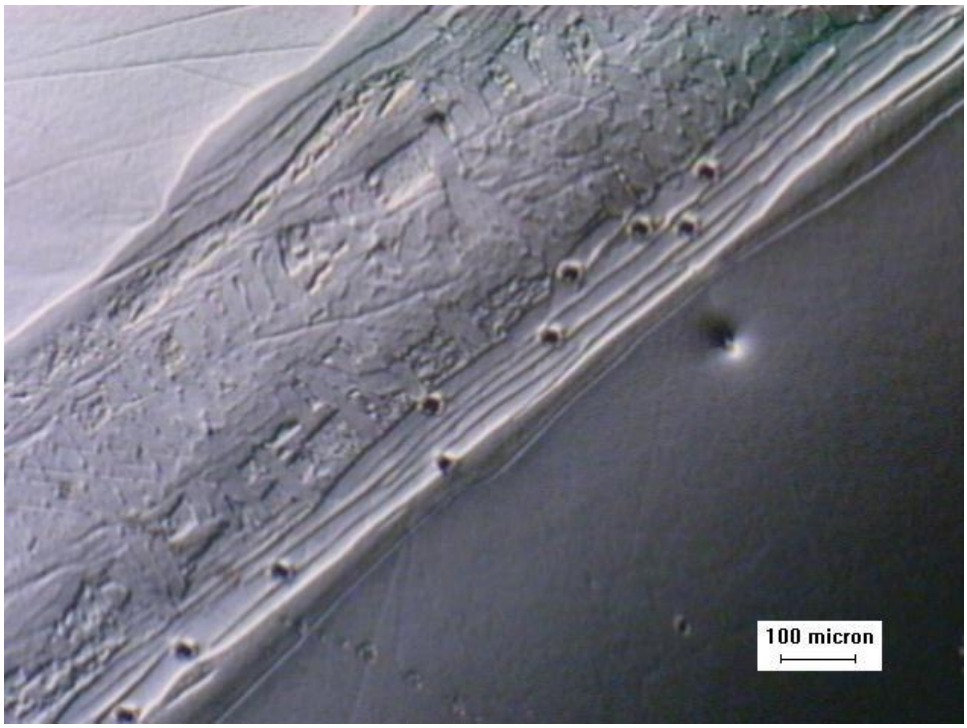

Figure 16: Vickers Hardness testing indents as seen on a secondary Widmanstätten ferrite plate at 100x magnification

From the results of the tests it can be seen that martensite has the hardest average value of 358.49, the secondary Widmanstätten ferrite has an average hardness value of 217.29 and the primary Widmanstätten ferrite has an average hardness value of 253.23. In order to better interpret the results from the hardness testing several plots were made to see if any trends existed. These can be seen in figure 17 through figure 19.

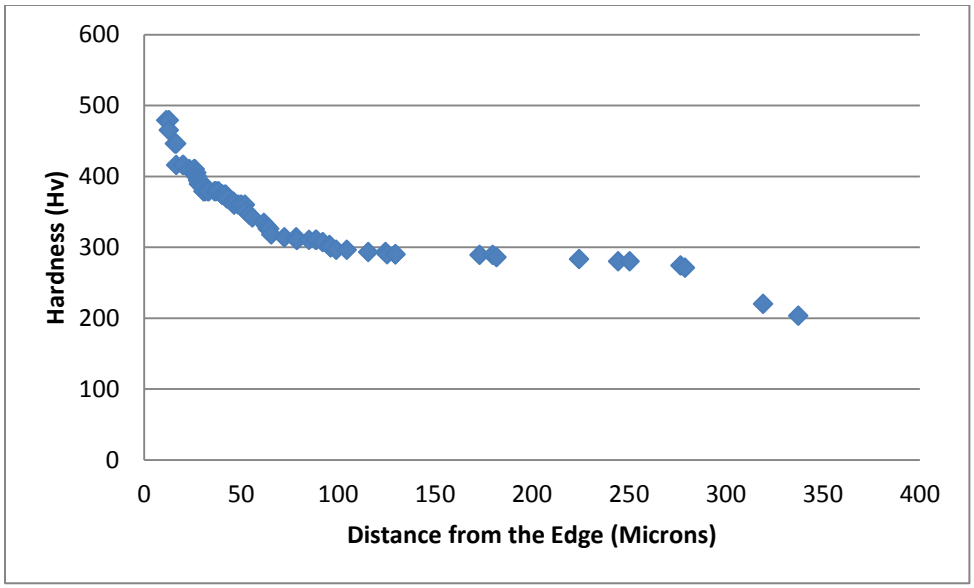

Fig 17: A plot of Vicker's hardness as a function of the distance of the indent from the edge of the plessite pool (martensite microstructure).

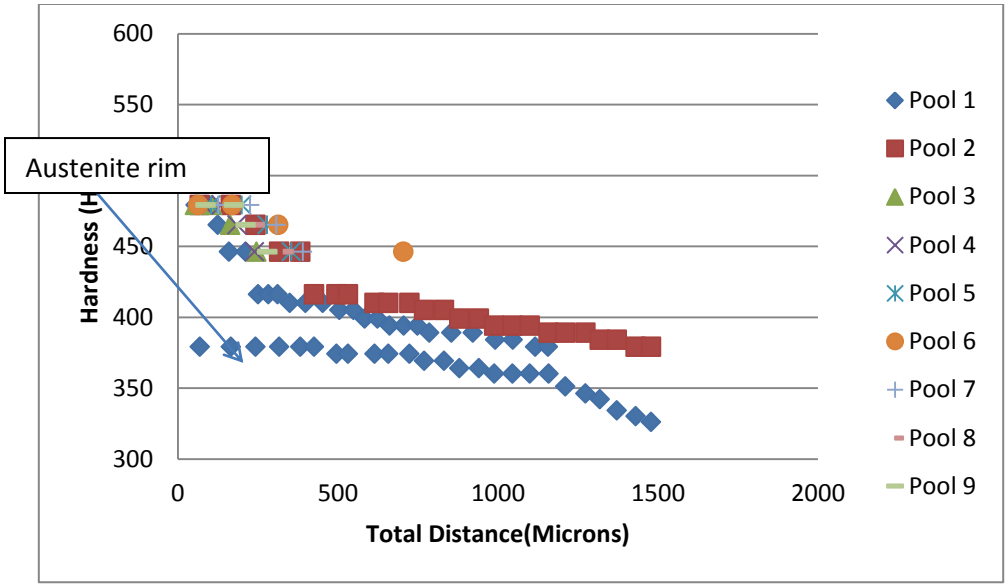

Fig 18: Vickers hardness as a function of distance for various plessite pools (martensite microstructure).

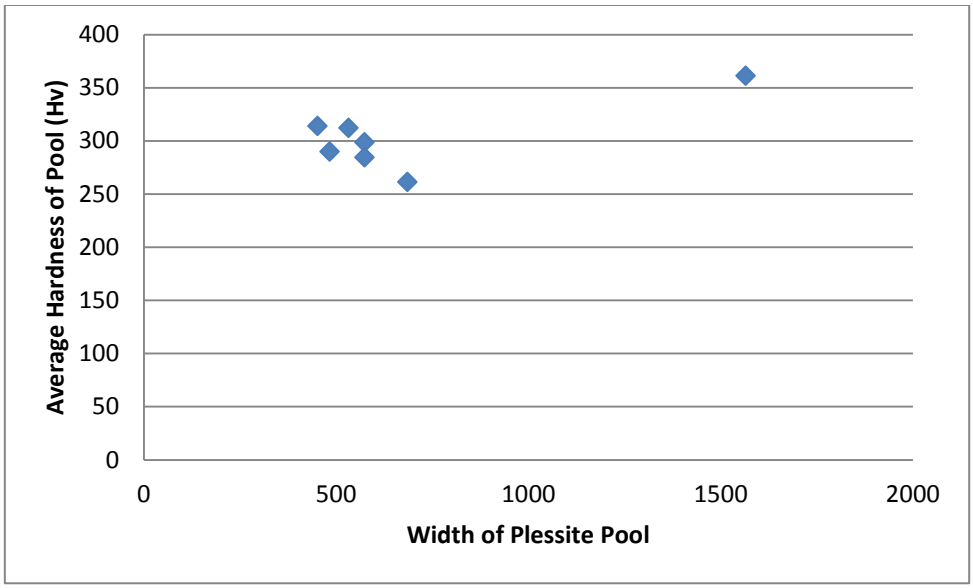

Fig 19: Average Vickers' hardness for each pool as a function of the width of the pool.

4.3 Conclusions

The goal of this thesis was to show that there was a difference in microhardness associated with primary Widmanstätten ferrite, secondary Widmanstätten ferrite, and martensite phases within the Cape York meteorite. While the difference between martensite and the Widmanstätten phases are significant, the differences within the Widmanstätten phases (primary and secondary) are less definitive. The secondary Widmanstätten ferrite results indicate that this phase is actually softer than the primary Widmanstätten ferrite which usually is not the case. It was observed in the Henbury meteorite that the opposite trend was true [30]. One theory that was developed to explain this phenomenon is that the secondary Widmanstätten ferrite formed later than the primary Widmanstätten ferrite and its growth was subsequently limited by the cooling process. Another theory is that small inclusions or subtle changes in the composition between the various meteorites could account for the primary Widmanstätten ferrite being harder than the secondary Widmanstätten ferrite.

It was also noticed from the data that martensite appears to be harder near the exterior of the home plessite pool. In figure 17 the origin indicates the "edge of the plessite pool". It is noticed that the regions which are closer to the edge of the pool the higher is its Vickers'

hardness. This is due to the higher Nickel content of the pool closer to the edge. This is further supported in Fig 18.

4.4 Future Work

In order to prove the reason for the primary Widmanstätten ferrite being harder than the secondary Widmanstätten ferrite a compositional analysis of these microstructures should be carried out. This could be done through EDS or other compositional analysis techniques. It is thought that this would show either higher nickel content in this region or a slight difference in composition which would explain the difference in hardness values between the two Widmanstätten ferrite structures.

Resources

[1] Kornreich, Dave. "Curious About Astronomy: Why Is It Important to Study Meteorites?" *Curious About Astronomy? Ask an Astronomer*. Mar. 1999. Web. 13 Sept. 2010. <http://curious.astro.cornell.edu/question.php?number=223>.

[2] Buchwald. V.F., Handbook of Iron Meteorites. 1975 Published for the center for the center for meteorite studies, Arizona State University. Published by the University of California Press.

[3] Williams, David R. "Evidence of Ancient Martian Life in Meteorite ALH84001?" *Welcome to the NSSDC!* 09 Jan. 2005. Web. 14 Sept. 2010. <http://nssdc.gsfc.nasa.gov/planetary/marslife.html>.

[4] "Meteors L Meteorites and Impacts." *The Nine Planets Solar System Tour*. Web. 01 Nov. 2010. <http://nineplanets.org/meteorites.html>.

[5] Yeomans, Donald K. "SENTRY - An Automatic Near-Earth Asteroid Collision Monitoring System." *Near-Earth Object Program*. 12 Mar. 2002. Web. 01 Nov. 2010. <http://neo.jpl.nasa.gov/news/news126.html>.

[6] "Asteroid - Definition and More from the Free Merriam-Webster Dictionary." *Merriam-Webster Online*. Web. 08 Sept. 2010. <http://www.merriam-webster.com/dictionary/asteroid>.

[7] Parsons, T., and J. Mackay. "Pièrre Simon Laplace: The Nebular Hypothesis." *Answers in Genesis - Creation, Evolution, Christian Apologetics*. Aug. 1980. Web. 08 Sept. 2010. <http://www.answersingenesis.org/creation/v3/i3/ideas.asp>.

[8] Francis, Eric M. "The Laws List: B." *Alcyone Systems*. 06 May 2010. Web. 08 Sept. 2010. <http://www.alcyone.com/max/physics/laws/b.html>.

[9] Ray Patrick C. “Microstructural Evolution of Iron Nickel Meteorites.” Pennsylvania State University. State College, Pennsylvania. 2007

[10] "Bode's Law." *Cornell Astronomy*. Web. 08 Sept. 2010. <http://www.astro.cornell.edu/academics/courses/astro2201/bodes_law.htm>.

[11] "Meteorite - Definition of Meteorite by the Free Online Dictionary, Thesaurus and Encyclopedia." *Dictionary, Encyclopedia and Thesaurus - The Free Dictionary*. Web. 08 Sept. 2010. <http://www.thefreedictionary.com/meteorite>.

[12] "Types of Meteorites." *The Meteorite Market*. Web. 21 Sept. 2010. <http://www.meteoritemarket.com/type.htm>.

[13] Amethyst Gallery, Inc. "Chondrites." *Amethyst Galleries' Mineral Gallery*. Web. 21 Sept. 2010. <http://www.galleries.com/rocks/chondrites.htm>.

[14] New England Meteoritical Services. *Meteorlab.com - Everything about Meteorites*. Web. 21 Sept. 2010. <http://www.meteorlab.com/METEORLAB2001dev/achonds.htm>.

[15] "Stony Iron-meteorites." *Haberer-Meteorite Geschenke Des Himmels*. Web. 21 Sept. 2010. <http://www.haberer-meteorite.de/english/Stone iron meteorites.htm#Pallasite>.

[16] Bottke, William F., and Linda M.V. Martel. "PSRD: Iron Meteorites as the Not-So-Distant Cousins of Earth." *Planetary Science Research Discoveries | PSRD*. 21 July 2006. Web. 21 Sept. 2010. <http://www.psrd.hawaii.edu/July06/asteroidGatecrashers.html>.

[17] "The Meteorite Museum - University of New Mexico." *EPS Homepage*. Web. 21 Sept. 2010. <http://epswww.unm.edu/meteoritemuseum/virtualtour/differentiated.htm>.

[18] "Meteorite.fr - Classification - Iron Meteorites - Main." *Meteorites*. Web. 21 Sept. 2010. <http://www.meteorite.ch/en/classification/ironmain.htm>.

[19] "Iron Metorite." *The Worlds of David Darling*. Web. 28 Sept. 2010. <http://www.daviddarling.info/encyclopedia/I/iron_meteorite.html>.

[20] Buchwald, Vagn Fabritius. "Chapter 9: The Minerals and Structural Components of Iron Meteorites." *Handbook of Iron Meteorites, Their History, Distribution, Composition, and Structure*. Berkeley: Published for the Center for Meteorite Studies, Arizona State University by the University of California, 1975. 87-120. Print.

[21] Taylor, G. J. "PSRD:: Asteroid Heating: A Shocking View." *Planetary Science Research Discoveries | PSRD*. 2 Apr. 2004. Web. 04 Oct. 2010. <http://www.psrd.hawaii.edu/April04/asteroidHeating.html>.

[22] Wittke, James. "Meteorite Book: Glossary P." *Welcome to Www4.nau.edu*. 08 June 2009. Web. 04 Oct. 2010. <http://www4.nau.edu/meteorite/Meteorite/Book-GlossaryP.html>.

[23] Cymru, Amgueddfa. "Meteorite Minerals | National Museum Wales." *Home | National Museum Wales*. Web. 05 Oct. 2010. <http://www.museumwales.ac.uk/en/837/>.

[24] "Martensite." *At the Sign of the Three Planes*. Web. 28 Sept. 2010. <http://www.threeplanes.net/martensite.html>.

[25] "Cape York Meteorite." *Wikipedia, the Free Encyclopedia*. Web. 11 Nov. 2010. <http://en.wikipedia.org/wiki/Cape_York_meteorite>.

[26] "CAPE YORK METEORITE CAPE YORK METEORITES." *METEORITES FOR SALE*. Web. 11 Nov. 2010. <http://www.arizonaskiesmeteorites.com/AZ_Skies_Links/Cape_York/>.

[27] "Arthur Ross Hall of Meteorites." *American Museum of Natural History*. Web. 11 Nov. 2010. <http://www.amnh.org/exhibitions/permanent/meteorites/what/capeyork.php>.

[28] R.L. Smith & G.E. Sandland, *An Accurate Method of Determining the Hardness of Metals, with Particular Reference to Those of a High Degree of Hardness*, Proceedings of the Institution of Mechanical Engineers, 1922, **1** p 623–641

[29] "Vickers Hardness Test." *Thermal Spray Coatings*. Web. 09 Dec. 2010. <http://www.gordonengland.co.uk/hardness/vickers.htm>.

[30] Dietz, Nicholas R. *Characterization of Widmanstätten Ferrite and Plessite in the Henbury Meteorite*. Print.